Astronomical and Astrophysical Transactions (*AApTr*), 2016, Vol. 29, Issue 2, pp. 109–128,
ISSN 1055-6796, Photocopying permitted by license only, ©Cambridge Scientific Publishers

Gamma-ray bursts appear simpler than expected?

Pascal Chardonnet[1,2,*], Anastasia A. Filina[1], Mikhail V. Popov[3],
Valery M. Chechetkin[2,4], Andrey A. Baranov[5]

[1]*LAPTh, Univ. de Savoie, CNRS, B.P. 110, Annecy-le-Vieux F-74941, France*
[2]*National Research Nuclear University MEPhI, 31 Kashirskoe Sh., Moscow 115409, Russia*
[3]*Ecole Normale Superieure de Lyon, CRAL, Univ. de Lyon 1, 46 allee d'Italie 69007 Lyon, France*
[4]*Keldysh Institute of Applied Mathematics, Russian Academy of Sciences, 4 Miusskaya Sq., 125047, Moscow, Russia*
[5]*National Research Centre "Kurchatov Institute", 1 Akademika Kurchatova Pl., 123182, Moscow, Russia*

Received 15 November, 2015

The cosmic gamma-ray bursts are certainly an enigma in astrophysics. The "standard fireball" scenario developed during many years has provided a possible explanation of this phenomenon. The aim of this work is simply to explore a new possible interpretation by developing a coherent scenario inside the global picture of stellar evolution. At the basis of our scenario is the fact that maybe we have not fully understood how the core of a pair instability supernovae explode. In such a way, we have proposed a new paradigm assuming that the core of such massive star, instead of doing a symmetrical explosion, is completely fragmented in hot spots of burning nuclear matter. We have tested our scenario using some observational data like GRB spectrum, light curves, Amati relation and GRB–SN connection, and for each set of data we have proposed a possible physical interpretation. We have also suggested some possible tests of this scenario by measurement at high redshift. If this scenario is correct, it tells us simply that cosmic gamma-ray bursts are simply a missing link in stellar evolution.

Keywords: Gamma-ray bursts; stellar evolution

1 An unusual explosion

I dedicated this talk to Evgenii Pavlovich Mazets (1929–2013) of the Ioffe Physical Technical Institute of Saint Petersburg, one of the most important pioneers in the physics of cosmic γ-ray bursts (GRBs), recalling the sentence of Lev Landau: "the

*Email: pascal.chardonnet@cern.ch

science allows us to discover and to understand the phenomena that the human mind would not be able to imagine".

GRBs, one of the great mysteries in astrophysics, were fortuitously discovered by the US VELA satellites, operated by Los Alamos National Laboratory, in 1967 [1, 2]. GRBs are sudden, intense flashes of gamma radiation characterized by very fast variability with time scales as short as milliseconds. The Sixties were crucial years in introducing X and γ-ray astronomy for scientific purpose. This field of research seemed promising in terms of scientific returns, and new techniques were developed to measure the obscured universe. The quasars and the pulsars were discovered at the same epoch and have been completely understood [3, 4]. It is also remarkable to notice that pair instability supernovae explosions were also imagined the year of the discovery of GRBs [5]. Until now, many scientists from around the world have built new experiments to study this enigmatic phenomenon, developing a multidisciplinary field that explores the origin of GRBs [6]. In those fifty years, there have been great advances in GRBs. Among these we can cite: BATSE experiment has shown that practically all GRB spectrum follows a phenomenological law called the BAND spectrum [7].

One important piece of the Rosetta Stone was discovered in February 1997. Launched six months before, the Dutch–Italian Satellite Beppo-SAX* observed the first afterglow of gamma-ray bursts [8]. The discovery of long-lived afterglow in X-rays, optical and radio and the direct determination of the distance revolutionized the field [9–12]. The existence of a counterpart opened a new area in the gamma-ray burst field. The measurement of the first redshift opened Pandora's box putting GRBs directly in the field of cosmology. These intense flashes of gamma radiation are at cosmological distances and as a consequence their energy could be as high as 10^{54} ergs. It is equivalent of a star like our Sun being converted into pure energy within a few seconds: GRBs are therefore the most powerful explosions in the universe.

Already, at the end of the 1990's, a GRB could be completely characterized by a small set of numbers provided we could estimate the redshift: its total isotropic **luminosity** $L_{\rm iso}$, a peak **energy spectrum** $E_{\rm peak}$ and a very short duration of the **prompt emission time** $\Delta t \sim 100$ seconds compared to the relatively long duration afterglow of up to years. However, the GRB lightcurves are very puzzling: no two are identical. In some sense, they are like fingerprints.

Many other experiments in space and on earth have also contributed to clarify the definition of a gamma-ray burst, at least from an experimental point of view. A very important connection between long duration GRBs and supernovae has long been established. The association was made observationally when within the error circle of GRB 980425 a bright and energetic supernova was found [13]. Initially it was considered by some as a chance coincidence, but in the spectra of subsequent long GRBs further supernova signatures were apparent; most famously in GRB 030329. While all long GRBs could be accompanied by a supernova, the reverse is not true. It is estimated that the core collapse supernovae are 1000–10000 times more frequent than GRBs. No supernovae have been so far associated with short-duration GRBs. GRB 060614 has a duration of 102 seconds, which classifies it as a long-duration GRB, but its temporal lag and peak luminosity fall entirely within the short-duration GRB subclass. It does not fit into any class.

*See: http://www.asdc.asi.it/bepposax/

Long GRBs tend to lie in small faint blue galaxies. Afterglow spectroscopy has shown that these galaxies have a lower ratio of metals to hydrogen than does our local neighbourhood in the Milky Way, possibly reaching as metal-poor content as 1/100 of the metallicity of the Sun [14]. From VLT observations at high resolution with FORS2 presented in Ref. [15] the authors have deduced that the site of the GRB 060505 is considerably different from the rest of the galaxy. It has intense star formation, low metallicity and young age. Host galaxies of long-duration GRBs have often been found to be faint irregular galaxies [16, 17]. Modjaz et al. have compared metallicities at the site of nearby type Ic supernovae which had no GRBs with the chemical abundances of nearby galaxies at the site of GRBs where SNe Ic were seen. They found that the progenitors of GRBs have systematically low metallicity [18].

A major related issue which is under discussion is if GRBs are unbiased tracers of star formation. Kistler et al. have found some evidence of enhanced evolution in the GRB rate with ∼4 times as many GRBs observed at $z \sim 4$ than expected from star formation measurements [19]. It is consistent with theoretical expectations from metallicity effects. The fact that such measurement contradicts that GRB rate traces the star formation history is another confirmation of the fact that the GRB–SN association is different from the one it is usually expected. GRBs are the result of formation of very massive stars and therefore the star formation rate should be different. An increase of GRB rate observed at high z is directly related to the prediction that we expect more GRBs at high z. GRB 050904 at a redshift $z = 6.29$ was discovered and observed by Swift and with a spectroscopic redshift from Subaru Telescope is the first gamma-ray burst to be identified from beyond the epoch of reionization. The burst is remarkable in two respects: first, it exhibits fast evolving X-ray and optical flares that peak simultaneously at $t \sim 470$ s in the observer's frame and may originate in the same emission region; second, its afterglow exhibits an accelerated decay in the near infrared from $t \sim 10^4$ s to $t \sim 3 \times 10^4$ s after the burst coincident with repeated and energetic X-ray flaring activity.

Although a lot of progress has been made in last few years, the origin of these explosions is still a great mystery in physics. This topic has focused the attention of the most powerful earth and space observatories. No two GRBs look the same, but there are features common to many X-rays afterglow. The Swift mission has discovered the transition from the prompt emission dominated phase to the afterglow: after the prompt phase the afterglow decays very steeply before flattening out to what is called the plateau phase. Then the light curve breaks to steeper decay. Striking features superposed on the steadily fading light, called X-ray flares, can be seen. X-ray flares can be very intense – once a giant flare containing almost as much energy as in the GRB itself was observed [20].

On the other hand, if great advances have been made from the theoretical point of view, the origins of GRBs are still a mystery. However, many models, when tested by experiment, have been abandoned and it is now well established that long GRB are related to the end of massive stars. Although it is true that many scientists favored the idea of the fireball, there is still no undisputed evidence for the GRB engine. **Any study of Gamma-Ray Bursts invites consideration of the factors that produce such exceptional events.**

2 Why gamma-ray bursts are as they are?

Soon after the 140th meeting of the American Astronomical Society, two theoretical papers proposed an explanation of the cosmic *gamma*-ray bursts. Colgate has shown that a pulse of gamma radiation is emitted when the shock breaks out of a supernova [21]. Bisnovaty-Kogan et al. proposed a similar conclusion [22]. The value of the pulse energy $\sim 10^{44}$ ergs and the typical energy of the photons $\sim$100 GeV were too far from observations. However, this idea was interesting: it was the first attempt to explain GRBs as a natural consequence of supernovae explosions. Now, after decades of observations, we understand why this scenario failed: GRBs are much more powerful than SN explosions and they radiate in X and γ radiation at the prompt phase. Instead, SN are less powerful and need time to radiate the huge amount of energy.

In the "Standard Model" of GRBs: the fireball and related scenario, the key idea is related to the ultra relativistic motion of a jet or a shell in expansion after the formation of a black hole [23–26]. In 2009, P. Chardonnet et al. proposed a new interpretation of gamma-ray bursts phenomenon inside a global picture of stellar evolution [27]. In the physics of stellar evolution, the mass is a key parameter that determines the fate of a star. We will assume that gamma-ray burst, as a star, follows also this simple principle: we argue that the main element of this concept is related to the mass of the progenitor. The first element which characterizes a GRB as an explosive event is huge amount of hard radiation released in a very short time. Paradoxically, such event exists inside the stellar evolution: it is the total disruption of a very massive star ongoing pair instability.

One of the first works that have considered electron–positron pairs creation inside stars and predicted instability caused by this process is the paper of W.A. Fowler and F. Hoyle [28]. Using polytropic structure approximation and the assumption that a star evolves through a series of quasi-equilibrium states, they have computed the density–temperature relations for massive stars taking into account variable number of electron–positron pairs. With these relations authors obtained evolutionary tracks of stars in a temperature–density plane. During evolution a star contracts and increases its central density and temperature. One of the most important obtained results is the fact that at temperatures about $1–3 \cdot 10^9$ K the energy gathered from the gravitational contraction of the star is not sufficient for creation of new electron–positron pairs, thus contraction starts to accelerate and implosion sets up.

Neutrino processes have been also examined by the authors and they have found that neutrino emission by electron–positron pair annihilation process $e^- + e^+ \rightarrow \nu + \bar{\nu}$ is the most part of neutrino losses. Neutrino losses highly affect evolution of a star at high temperatures.

Later it has been proved by detailed evolutionary computations that in stars heavier than 20–30 $M_\odot$ the pair-creation process leads to development of dynamical instability [29]. Pair-creation can be also described in terms of the adiabatic index γ: this process reduces γ to the values less than 4/3, which is the critical value for dynamical stability of a star.

First dynamical calculations of explosion triggered by pair-creation instability have been performed by Barkat, Rakavy and Sack [5]. They have used the 40 $M_\odot$ oxygen star model and have found that after reaching dynamical instability the star started to contract with acceleration. Explosive nuclear burning in the center released energy

corresponding to consumption of several solar masses of oxygen (the obtained value was $\sim 6 \times 10^{51}$ ergs). This reversed the collapse and leads to total disruption of the star without any remnant. "This is despite the fact that during collapse the imbalance between the gravitational forces and the thermal pressure gradients is only about 1% and thus induces very small accelerations." The authors have checked the influence of admixture of carbon, effect of outer layers of lighter matter, but behavior remained the same as for pure oxygen 40 $M_\odot$ star. The authors also have made the attempt to investigate conditions in which pair-instability is possible; and they have found the limit on the mass of the oxygen core of 30 $M_\odot$. The cores lighter than this limit passed pair-instability zone and evolved up to Fe–He transition region. The 30 $M_\odot$ oxygen core entered into regime of decaying oscillations.

In the following years the investigation of stellar evolution and dynamical behavior of pair-unstable stars was continued. Evolution of carbon–oxygen stars with different masses has been studied by numerical calculations [30] and isentropic analytical models [31]. The authors have concluded that stars heavier than 25 $M_\odot$ are dynamically unstable because of pair-production. Instability occurs before ignition of oxygen. In Ref. [32] Fraley performed numerical calculations of the oxygen cores with masses of 45, 52 and 60 $M_\odot$. Oscillations were found for the 45 $M_\odot$ core, while the other two exploded without remnant. Simulations for higher mass range have been done by Arnett. He evolved helium cores with masses 64 and 100 $M_\odot$, which corresponded to 58 and 93 $M_\odot$ oxygen cores. Explosion was found for both cases. Wheeler has performed computations for 10^3 and 10^4 $M_\odot$ oxygen cores [33]. Both of them collapsed to black holes without mass ejection despite nuclear burning during collapse. All these computational experiments, disagreeing in detailed values, have demonstrated the main feature: with low masses of oxygen core stars oscillate, don't disrupt totally; heavy oxygen cores collapse to black holes without mass ejection; in the middle mass range stars produce very energetic explosions that reverses the collapse and disrupts the star.

El Eid, Fricke and Ober have studied detailed evolution of stars with initial masses of 80–500 $M_\odot$ that consist of hydrogen and helium (model of Population III stars) [34]. They have shown that at the end of helium burning stage stars consist mainly of carbon and oxygen ($\sim$90% of the mass). Stars with initial mass higher than 100 $M_\odot$ evolve very rapidly after helium burning and enter the electron–positron pair creation region. The authors used these carbon–oxygen cores as initial configurations for further hydrodynamical calculations [35]. They have found that carbon–oxygen cores with mass within 48–112 $M_\odot$ explode and heavier cores collapse. This result is in agreement with the upper mass limit of 100 $M_\odot$ for explosion of oxygen cores obtained by Bond, Arnett and Carr [36].

The effect of rotation on evolution of massive carbon–oxygen cores in rigid-body approximation has been considered in Ref. [37]. In this paper authors have shown that rotation could expand the region of explosion to higher masses.

We have computed dynamics of unstable massive oxygen cores by solving system of hydrodynamical equations in the Lagrangian variables under assumption of spherical symmetry [38]. We have performed the hydrodynamical simulations for the several models of stars with different masses M of the core. We considered only the cores with initial composition assumed to be pure oxygen. Initial configurations were computed from the hydrostatic equilibrium condition with the polytropic index $n = 3$.

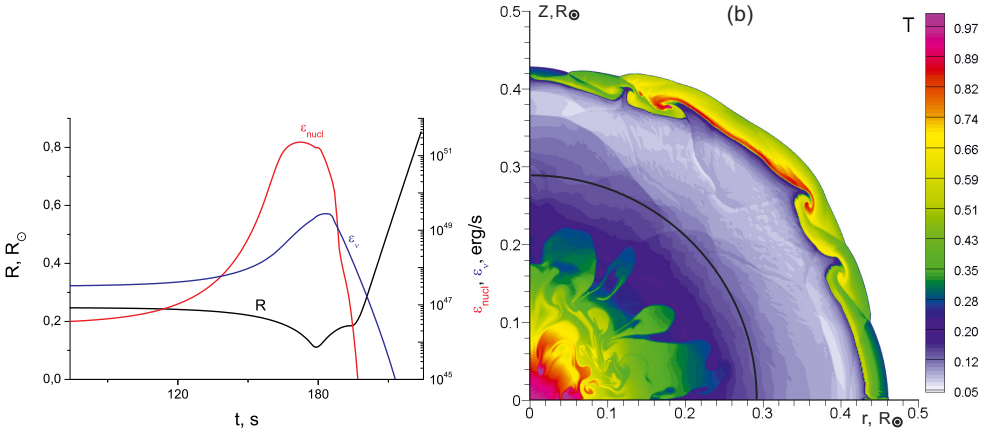


Figure 1 Left: 1D hydrodynamical code showing the results of the explosion of 100 $M_\odot$ oxygen core. r is the radius of the core, $\varepsilon_{\rm nucl}^{\rm tot}$ is the rate of total nuclear energy production, $\varepsilon_\nu^{\rm tot}$ is the total neutrino losses. Right: 2D hydrodynamical code showing the values of T in logarithm scale in units of 2.36×10^9 K and the fragmentation of the core [38].

It is seen from the results of numerical simulations that for more massive cores higher maximum temperatures, $T_{\rm max}$, are reached. As a result, more nuclear energy, $E_{\rm nucl}$, is emitted. There is definitely a correlation between these values. There is more nuclear fuel in more massive cores and it is more difficult to reverse collapse of such cores, so they contract stronger. But at high enough temperatures endothermic photo-disintegration of heavy nuclei becomes more effective and reduces the pressure inside a star, favoring collapse of more massive cores. An example of such simulations is presented in Fig. 1: the radius of the core, r, absolute value of the total neutrino losses, $\varepsilon_\nu^{\rm tot}$, and nuclear energy production rate, $\varepsilon_{\rm nucl}^{\rm tot}$, in a whole star are shown as functions of time. This simulation was made for the 100 $M_\odot$ oxygen core with initial central density $2.65 \cdot 10^5$ g/cc and temperature $2.36 \cdot 10^9$ K. The key to understanding the energy budget $E_{\rm nucl}$ in PISNe is related to the nuclear energy burning:

$$E_{\rm nucl} \sim M_c \times q, \tag{1}$$

where q is the energy rate per gram produced by nuclear reactions where $q \simeq 6 \times 10^{17}$ erg·g^{-1} [28]. The more massive the star is, the more energetic the explosion will be. We have found that the timescale is also compatible with GRBs. The star is totally disrupted in few ∼10 seconds. One of the important points here is that temperature of stellar matter heated by nuclear burning reaches the maximum values in the range of 100–500 keV. In the case of total disruption of the star hot matter of the core could be ejected outside. And energy gathered from nuclear burning will be emitted by electromagnetic radiation with the same characteristic energies. The efficiency of transformation of the nuclear energy to emission should be high, since there are no intermediate processes of transformation and redistribution of energy.

We have proposed a new paradigm related to the fragmentation of the core during the explosion of very massive stars [38]. This could be the result of large scale convection inside the core just before the explosion. Figure 1 represents the fragmentation of the core after the explosion. We can conclude that the prompt emission is certainly

related to the total disruption of a very massive star through pair instability process. The prompt emission consists of the X-γ radiation emitted by the nuclear explosive process of very massive core. Due to the total disruption of the star, the efficiency could be very high: we can construct a scenario where this prodigious hard radiation is emitted without significant absorption.

3 A unified picture of gamma-ray bursts

In this part, we will present a physical and coherent explanation of some main results of GRBs.

The Amati Relation is a mysterious relation between the isotropic energy $E_{\rm iso}$ and the peak energy spectrum $E_{\rm peak}$ obtained for GRBs using different satellites. So, it certainly contains some common physical properties of the engine, despite the apparent diversity.

The second relation is the Band spectrum of GRBs. This law represents the most successful way of fitting GRB spectrum. Certainly $E_{\rm peak}$ represents some fundamental property of GRB physical emission processes. And again, as for the Amati relation, this law is valid for numerous GRBs independent of the other parameters observed in GRB that could have different values.

We believed that these two laws certainly contain some key to understanding the physics of GRBs. Then we will analyse the GRB lightcurves. Contrary to the spectrum, each GRB has a specific imprint which is its lightcurve. We will propose a new physical understanding of this diversity.

Finally we will show that the GRB–SN connection could be also easily understood in terms of mass using the Salpeter function and we give a possible explanation of the unexpected rise in the GRB rate with redshift observed by Swift.

3.1 The Amati relation

In 2002 Amati and co-authors discovered a correlation between the estimated total isotropic energy, $E_{\rm iso}$, and the associated peak energy $E_{\rm p}$ [39]. Since then many authors have proposed possible explanations inside the fireball model of GRBs. We can notice that all these interpretations assume parameters. Following our computation on pair instability we propose a new interpretation of the Amati Relation based on a single parameter: the mass M of the progenitor star [40].

To understand our new interpretation it is necessary to recall an important fact related to GRBs. Many studies of GRBs spectrum have shown that the energy peak of emission, $E_{\rm peak}$, is at values $\sim$100 keV [42]. Up to now the very high energy emission (TeV photons) in GRBs has not been observed. The GeV emission is associated only with a small number of GRBs.

This observational fact is essential. It is a statistical measure made on different GRBs showing a common central value of $E_{\rm peak}$ despite the diversity of other measurements. If we read this value in equivalent of temperature it means simply that $E_{\rm peak} \sim 10^9$ K. According to us, this is the first key reading in order to understand the Amati relation: to interpret $E_{\rm peak}$ in terms of temperature. The second key reading is now straightforward. In our interpretation of GRBs, using pair-instability

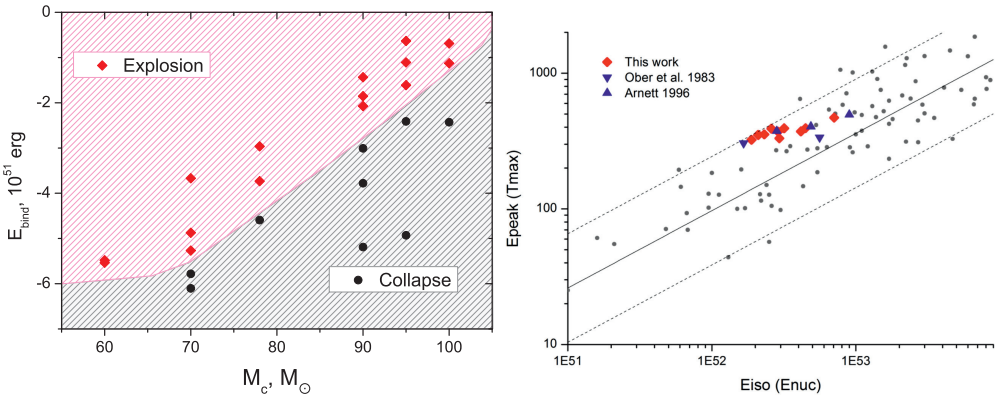


Figure 2 Left: Fate of a star depending on its core mass and binding energy. Explosion is marked by diamonds and collapse by circles. Right: Nuclear energy release as a function of the maximum temperature surmised on the diagram of the Amati relation points. Our computation assumes only the mass as parameter of the progenitor as parameter. No other fitting parameter has been used [38].

supernovae, this is a direct consequence of the temperature of nuclear burning of the matter at the instant of explosion of the star: $T_{\max} \sim 100$ keV, which is precisely the same order of $E_{\rm p}$. Now assuming that the progenitor of GRB is a very massive star ongoing pair instability explosion, we naturally associate the peak energy $E_{\rm p}$ with the $T_{\max}$, and the total isotropic energy $E_{\rm iso}$ with the nuclear energy reservoir $E_{\rm nucl}$ at the instant of the explosion. Figure 2 shows that in this case computed values perfectly fit inside the area of observable data [43].

This physical interpretation of the Amati Relation enlightens us about the key parameter of GRBs: the mass of the progenitor M. The nuclear energy reservoir $E_{\rm nucl}$ is in perfect agreement with the isotropic energy $E_{\rm iso}$. In short, the Amati Relation tells us that the more massive the progenitor of GRB is, the higher the peak energy $E_{\rm p}$ is, and the more significant the total isotropic energy $E_{\rm iso}$ will be. Recalling that the first simulation of PISNe done by [29] have shown that a 40 $M_\odot$ produces $\sim 6. \times 10^{51}$ ergs, we see also that the lower part of the Amati diagram could be also covered by low mass star progenitors. And following the results of Glatzel et al., we point out that the rotation could allow for stars more massive than 120 $M_\odot$ to explode in pair instability process [37]. This point is certainly very important for primordial stars, population III, where the mass could be as high as 500 $M_\odot$. In this case we expect very powerful GRBs with higher value of peak energy $E_{\rm p}$. According to our idea, the Amati diagram is simply reading of the usual window of PISNe in terms of progenitor mass with the transformation law $(E_{\rm peak}, E_{\rm iso}) \rightarrow (E_{\rm nucl}, T)$. **It is quite remarkable that to reproduce the Amati relation we need only the progenitor mass and no other fitting parameters are needed.** However, the most extraordinary is that, perhaps, the physical explanation of this apparent mysterious relation is simply related to standard stellar physics equations:

$$\frac{dT}{dr} = \frac{3\kappa\rho L}{16\pi acT^3 r^2}. \tag{2}$$

Using the $E_{\rm nucl} \sim M_c \times q$ and $\dfrac{dT}{dr} \sim \dfrac{T}{r}$ with the definition of $\rho \sim \dfrac{M}{r^3}$ we can derive the famous Amati relation dependence using our set of parameters $(E_{\rm nucl}, T)$:

$$T^2 \sim E_{\rm nucl}. \tag{3}$$

We have also tried to understand the dispersion observed in the Amati Relation. In our interpretation the distribution of the points on $E_{\rm p}$–$E_{\rm iso}$ diagram corresponds to window of physical parameters of a massive star required for pair-instability explosion. Different chemical compositions give different temperatures of nuclear burning and different energy production. If the star is composed of silicon, the explosive burning will happen at higher temperatures than for composition of pure oxygen. The metallicity is certainly another key parameter and more simulations should be done.

3.2 The spectrum

In 1993, Band proposed a phenomenological law to interpret almost all the GRB spectrum with a simple form [7]:

$$N_{\rm B}(E) = \begin{cases} CE^{\alpha}e^{-E/E_0}, & (\alpha-\beta)E_0 \geq E, \\ C'E^{\beta}, & (\alpha-\beta)E_0 < E, \end{cases} \tag{4}$$

where $N_{\rm B}(E)$ is the photon number spectrum, E is the photon energy in keV, E_0 is the e-folding energy, α and β are the asymptotic power-law indices, C is the amplitude in photons s^{-1} cm^{-2} keV^{-1} and C' is chosen to make $N_{\rm B}(E)$ a continuous and continuously differentiable function: $C' = C\left((\alpha-\beta)E_0\right)^{\alpha-\beta} e^{-(\alpha-\beta)}$. Spectral hardness is usually measured by the peak energy $E_{\rm peak}$ of the EF_E spectrum ($F_E = EN_{\rm B}$). This energy is related to E_0 as $E_{\rm peak} = (2+\alpha)E_0$ and $(\alpha-\beta)E_0 = E_{\rm break}$.

If our interpretation of the Amati Relation is correct, it means that the environment of the GRB is composed of a very hot plasma $T \sim 10^9$ K essentially thermalized that could be described by a Planck function (Black-Body emission): $N_{\rm BB}(E) = A_{\rm BB}\,\dfrac{E^2}{e^{E/kT}-1}$, where $A_{\rm BB}$ is a normalization factor which depends on the area of the emission surface and the distance to observer. However, we know also, that a huge number of electrons, positrons and ions will be present during the explosion of the stars. Therefore, in addition to a thermal component it is also natural to assume a thermal bremsstrahlung part $N_{\rm Br}(E) = A_{\rm Br}\,\dfrac{1}{E}\,e^{-E/kT}$, where $A_{\rm Br}$ is a normalization factor. Thermal bremsstrahlung naturally explains $N_E \propto E^{-1}$ low-energy slope observed in many bursts [45].

The resulting spectrum is thus the sum of two contributions:

$$N(E) = N_{\rm BB}(E) + N_{\rm Br}(E) = A_{\rm BB}\,\frac{E^2}{e^{E/kT}-1} + A_{\rm Br}\,\frac{1}{E}\,e^{-E/kT}. \tag{5}$$

The detailed explanation using our hydrodynamical code is not the object of this work. However, we can say that regions with lower density radiate thermal bremsstrahlung spectrum owing to interaction of ionized electrons with protons and ions. Thermal bremsstrahlung is responsible for formation of low-energy part of GRB

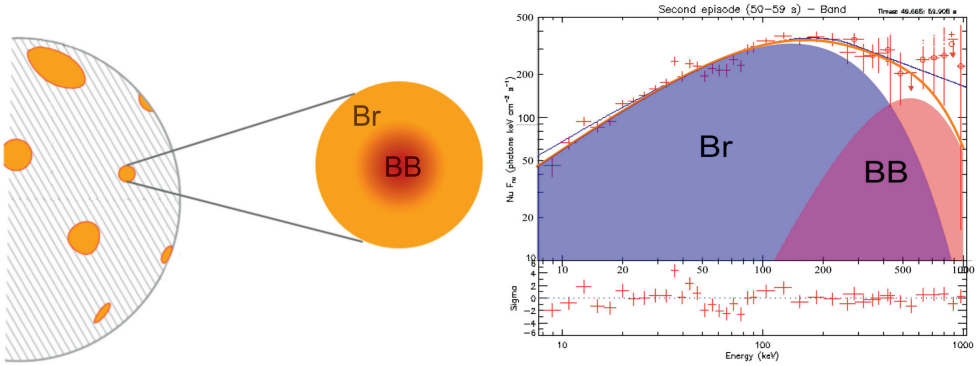


Figure 3 Left: Cartoon representation of a possible emission mechanism with Black-Body + Bremmsstrahlung emission. Our GRB spectra modeling is using Black-Body (BB) + Bremsstrahlung (Br). Hot spots randomly appear on the surface of exploding star. Right: Fitting of the GRB 090618 showing the repartition between Black-Body (BB) + Bremsstrahlung (Br) emissions.

spectrum. The central part of GRB spectrum in our model is dominated by thermal emission from the regions with higher density. In the first decade of GRB observations, their spectra appeared to be well fitted by thermal bremsstrahlung with temperature of ∼100 keV [51]. The thermal bremsstrahlung spectrum of the radiated energy can be described as [46]:

$$I_{\rm Br}(E) = n_e n_i \frac{32}{3} \left(\frac{\pi}{3}\right)^{1/2} \frac{e^4}{m_e^2 c^4} \left(\frac{Ry}{kT}\right)^{1/2} e^{-E/kT}\, \bar{g}, \tag{6}$$

where $I_{\rm Br}$ is the power emitted per unit volume per unit of time per unit energy, n_e and n_i are the number densities of electrons and protons, E is the photon energy, T is the electron temperature, Ry is the Rydberg energy constant, $\bar{g}$ is the Gaunt factor. For the task of spectrum fitting it is convenient to express I_E in physical units:

$$I_{\rm Br}(E) = 2 \times 10^{-20} \frac{n_e n_i}{\sqrt{T}}\, e^{-E/kT}\, \bar{g} \quad \frac{\rm erg}{\rm s \cdot cm^3 \cdot keV}. \tag{7}$$

Then the photon number spectrum measured by the observer is: $N_{\rm Br}(E) = \dfrac{I_{\rm Br}(E) V}{4\pi\, E\, D^2}$, where V is the volume of the emitting region, D is the distance towards the observer. This simple relation explains why this scenario was rejected for GRB spectra in the case of neutron star scenario in the 1980's [52]. Accretion on NS scenario used a volume V, too small in order to reproduce the observed spectra. Here, instead in the very massive star scenario the huge mass and large volume guarantee enough matter to radiate. Another criticism at that time was also the fact that in this NS model, magnetic fields were high enough that Bremsstrahlung was in direct competition with more efficient synchrotron emission.

Our result presented in Figure 3 represents a very good fit of GRB090618 where we have used both Black-Body and thermal Bremsstrahlung. This result tells us that the environment of the GRB engine should be very hot, ∼100 keV. From this first

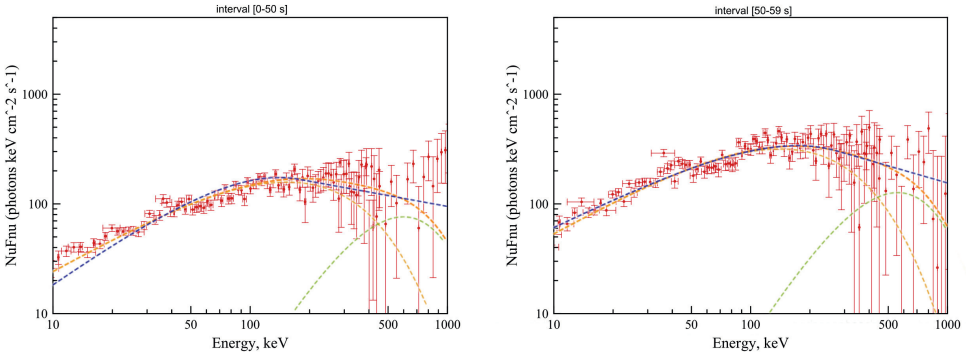


Figure 4 Time-integrated spectra for the different time intervals: from 0 to 50 s and from 50 to 59 s, after the trigger time of GRB 090618. Blue line shows the fit with the Band function (Eq 4), orange line shows the Black-Body (green dashed line) + bremsstrahlung (orange dashed line) (Eq. 5).

result we do expect to have a hot plasma cooling quickly. We notice also that at low energy ∼1 keV the GRB spectrum is due essentially to the bremsstrahlung.

Now if we look at the time dependence we have also succeeded in obtaining a very good result (Figure 4). We also have analyzed several other bursts and succeeded in reproducing the spectrum [41].

It is well known that GRB spectra are characterized by hard to soft emission. In our interpretation the hard part of the spectrum corresponds to the thermal Black-Body emission while the soft part is related to the thermal bremsstrahlung. This difference tells us also about the thickness of the emission region: the thermal emission is coming from thick region while the Bremsstrahlung emission from the thin regions. This result should be kept in mind for a dynamical point of view. It is well known that GRB spectrum emission presents a hard to soft characteristic. In view of our result, a possibility could be that dense regions, more thick, emit first a thermal emission and with time, due to some fast expansion, there are less dense regions and therefore a thermal Bremsstrahlung emission could be produced.

Bremsstrahlung works out very well. In hot thermal plasma we naturally expect to have copious photons emitted by black body emission and by thermal bremsstrahlung depending on thickness. Almost all GRB spectra present a turn-off called $E_{\rm peak}$ in the BAND terminology, where we have $E_{\rm peak} \sim kT$. If we assume that this model correct we do expect a very hot thermal plasma. **In hot thermal plasma where many heavy elements are present abundantly, we expect in addition to thermal bremsstrahlung to have also lines. These lines may be difficult to detect now but there could be an additional proof of the bremsstrahlung emission.**

3.3 The light curves

It has been noticed for some times that GRB spectra are more complex due to time variability [53]. Therefore, we have applied our combined fit (black-body + thermal

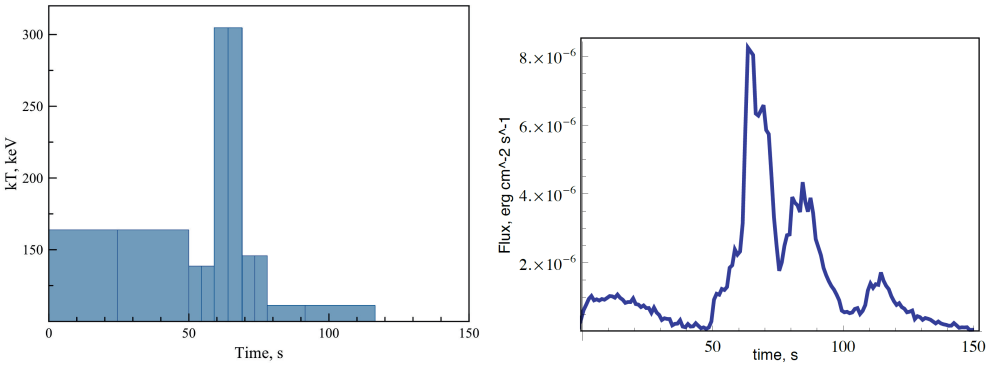


Figure 5 Left: Temperature evolution with time $T(t)$ of GRB 090618. Right: The light curve of GRB 090618 [48].

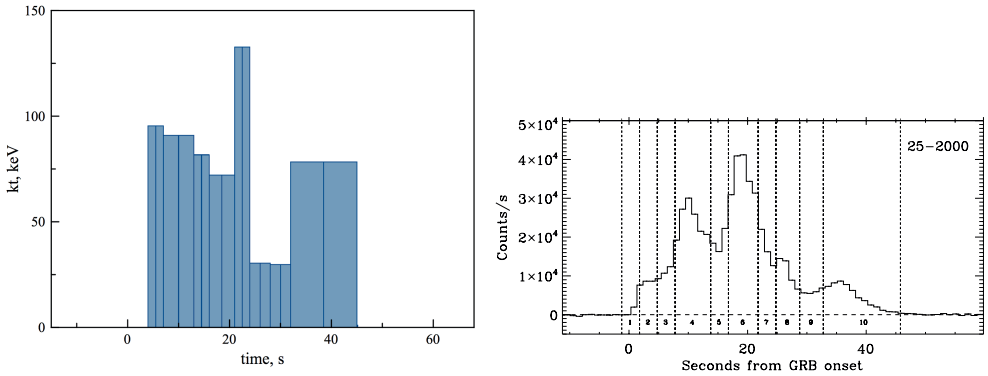


Figure 6 Left: Temperature evolution with time $T(t)$ of GRB 970111. Right: The light curve of GRB GRB 970111 [49].

Bremsstrahlung) with time-sequence analysis of GRB090618. We have analyzed the variation of the temperature with time and we have found that $T(t)$ is not a monotonic variation of time. Figures 5 and 6 show the variation in temperature of the hot plasma with time in correlation the associated light curve of this GRB.

Therefore, we have found the important result that the temperature is correlated in the same way as the variation of the light curve. We have also tested this result on other GRBs. We have also computed a radius associated to the black-body emission. This radius is very small $\sim 10^8$ cm. This radius is an equivalent radius for a BB emission. The dynamical radius which corresponds to hydrodynamical process related to the explosion is certainly much larger. **As a consequence of our model, we can conclude that the BB emission is not uniform on a unique surface but only bright hot spots emit located on a sphere with larger radius (see Figures 3 and 7).** Here, we have assumed uniform density of electrons and ions and will take a constant radius for duration of spectrum. In add we have assumed identical temperature for electrons and ions. With this crude assumption, the density derived are consistent with values of stellar explosion. The correct picture

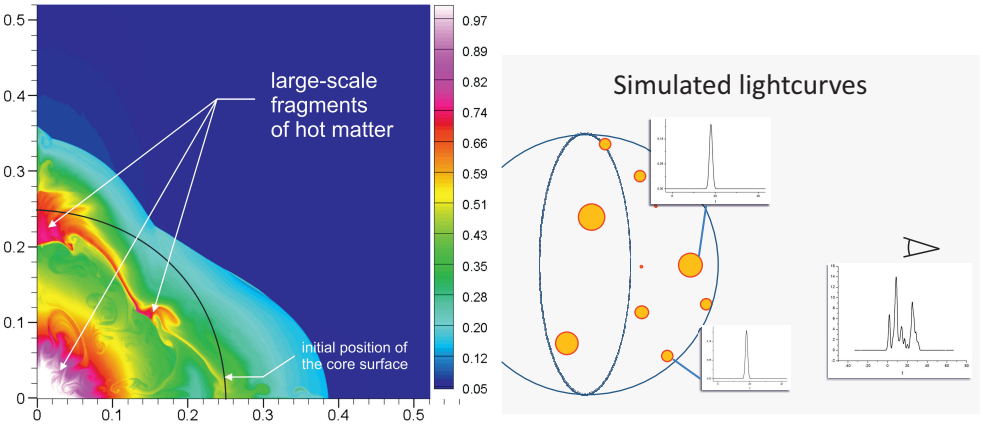


Figure 7 Left: 2D simulation of an explosion of a 100 solar mass pair instability supernovae explosion in the multicore explosion scenario using PPML methods. This picture shows the fragmentation of the core and hot spot regions of very high temperature. Right: Cartoon representation of a possible emission mechanism with Black-Body + Bremsstrahlung emission. Hot spots randomly appear on the surface of exploding star. Each spot produces spike of emission. Signals from these spots arrive at different times, so an observer sees the superposition of the spikes.

is certainly more complex with non uniform density and with possible clumps. But this is out of the scope of this paper. Following our time-resolved spectra analysis we expect that the temperature introduced in our first conclusion is correlated in the same way as the variation of the light curve. We have analyzed also: GRB990510, 980329, 101023 and 090926A. The conclusions are the same: the variation of T, in our model of BB+thermal Bremsstrahlung is correlated with the variation of the flux in the light curve.

Our result is a natural consequence of the previous results for time-resolved and time-integrated spectra. According to us, this result is very important since it establishes a physical link between one parameter of the spectra: the peak energy, and another parameter of the light curve: the maximum flux. We have shown that this link is valid even for a time-resolved spectra. The physical consequence, independent of any model, is important because this is a bridge between the two sets of data: light curves and spectra. The simplicity of the spectra through the phenomenological modeling with BAND spectrum is certainly related to a simple emission mechanism. On the other hand, the complexity of the light curve should also incorporate this simple emission mechanism. **We need to consider the light curve not as a whole complex structure but as complex superposition of simple structures: individual spikes with the same emission mechanism, which being applied to entire light curve works also. In short, a GRB light curve could be the result of many secondary sources.**

According to our spectra analysis we expect to have zones in the hot spots depending on density: the core, a thick region, is associated to BB emission while the output region of these blobs less dense, corresponding to Bremsstrahlung emission as we proposed in Figure 7. Our scenario is similar to many secondary sources which

originated from the initial destruction of the star. Here we have used a simple function in time $I_i = I_{0,i}\, e^{-(t-t_{0,i})^2}$ for the luminosity function of each blob. Here I_i is the intensity, $I_{0,i}$ is normalization factor, which is assumed to be proportional to the size of a spot i; $t_{0,i}$ is the time delay of arrival of a signal to observer, which depends on position of a spot on the surface. This simple function shows that the light curve of the burst could be explained by the sum (superposition) of the individual light curve $I = \sum_i I_i$. If this analysis is correct, it means that the prompt GRB emission is characterized by the typical timescales: the one of each spike related to the burning time $\tau_{\rm b}$ of the hot blob and the "propagation timescale" Δt related to the geometry of the different blobs as seen in Figure 7. If we take a burning blob of mass ΔM composed of Carbon with associated energy rate q, then the nuclear energy released ΔE could be written as follows: $\Delta E = q \times \dfrac{dY_C}{dt} \times \tau_{\rm b} \times \Delta M$, where $\tau_{\rm b}$ is the burning timescale. This burning time is very sensitive to the temperature and during the explosion, depending also on the value of ΔM, this burning time could be very short, compatible with the typical timescale of the spike [56]. The propagation timescale Δt is simply related to the geometry and it gives us an order of duration for long GRB since $\Delta t \sim \dfrac{R}{c}$, where R is the size of the external part of the star just after the explosion when the hot spots are reaching the surface and emitting. This tells us that a prompt duration of 10 seconds is associated with a typical size of $\sim 3 \times 10^{12}$ cm. This size is really compatible with the explosion of a very massive star. Moreover, we can also conclude why the duration of long GRB are statistically of order of $\sim$100 s, it is related to the size of the star.

3.4 The rate of GRBs in astrophysics and cosmology

In this part we have estimated the ratio of GRBs to that of SN Ibc and the rate of GRBs as the function of redshift.

The small number of GRBs in relation to the total number of SN Ibc observed is, again, a natural consequence of the very massive progenitor mass. Using Salpeter function and assuming a typical GRB progenitor of 100 $M_\odot$ and 20 $M_\odot$ for a SN Ibc, we can deduce that this rate is proportional to $\left(\dfrac{M_{\rm GRB}}{M_{\rm SN}}\right)^{-2.5} \sim 0.4\%$. This rate is in agreement with the one derived by M. Della Valle [57].

Now, regarding the rate of GRB with redshift, we will assume that GRBs are related to Pair-Instability Supernovae. To find a number of observed GRBs with redshift in $(z, z + dz)$ over a time interval dt

$$\frac{dN_{\rm GRB}}{d\,z} = \frac{\Omega_{\rm obs}}{4\pi} \cdot P_z \cdot R_{\rm grb}(z) \cdot \frac{dt}{1+z} \cdot \frac{dV}{dz}(z) \cdot \int \Phi(L) d\log L. \tag{8}$$

In this equation there are two unknown functions: luminosity function $\Phi(L)$ and rate of GRB $R_{\rm GRB}(z)$. The other parameters are the following: $\Omega_{\rm obs}$ – field of view of experiment, $\Omega_{\rm obs} = 1.4$ for Swift, $P_z = 0.28$ – normalization factor, dt – observation time, $\dfrac{dV}{dz}(z)$ – comoving volume element per unit of redshift.

$$\frac{dV}{dz}(z) = c \cdot \frac{4\pi d_L^2(z)}{H(z) \cdot (1+z)^2},$$

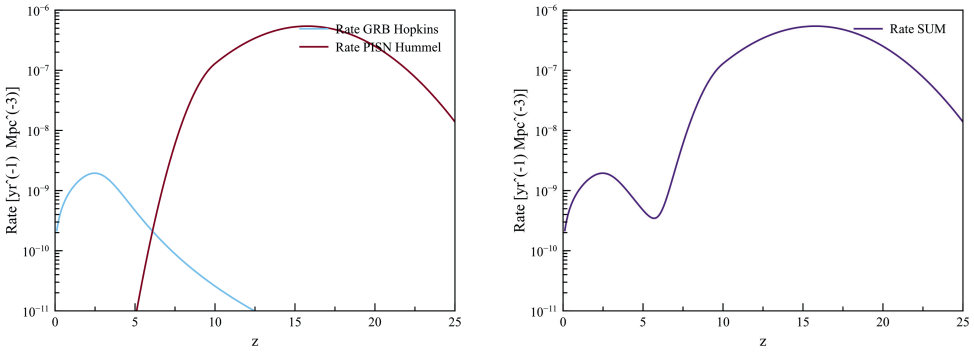


Figure 8 Left: Rate GRB from [60] and rate PISN from [61]. Right: Sum of rate GRB from [60] and rate PISN from [61].

c – speed of light 299 792 458 m/s, $d_{\rm L}$ – luminosity distance [Mpc], $H(z) = H_0 \cdot ((\Omega_L + \Omega_K \cdot (1+z)^2 + \Omega_M \cdot (1+z)^3 + \Omega_R \cdot (1+z)^4)^{1/2}$, $H_0 = 72$ [km·c^{-1}· Mpc^{-1}] – Hubble constant, $\Omega_{\rm L} = 0.73, \Omega_M = 0.27, \Omega_R = 0, \Omega_K = 0$ – cosmological parameters. The luminosity function $\Phi(L)$ can be calculated in different ways [58, 59]. To compute the number of GRBs per redshift, it is necessary to know the rate of GRB per unit of volume, $R_{\rm GRB}$. Number of observed GRBs is proportional to the rate of GRB as function of redshift, comoving volume and observational time. It is necessary to have a model that can define $R_{\rm GRB}$. One of the standard approaches is to assume that the rate of GRB is proportional to the star formation rate.

But we also assumed that the rate of GRBs can be proportional to the rate of pair-instability supernova. Let's consider $R_{\rm GRB}(z)$ – rate of GRB. There are different ways too. Generally it is assumed that the rate of GRB is proportional to star formation rate $R_{\rm SFR}(z)$: $R_{\rm GRB}(z) = k_{\rm GRB} \cdot R_{\rm SFR}(z)$. For SFR we used approximation formula by [60]: $R_{\rm SFR}(z) = \dfrac{(a_1 + a_2 \cdot z) \cdot h}{1 + (\frac{z}{a_3})^{a_4}}$, with: a_1, a_2, a_3, a_4, h – parameters $a_1 = 0.017, a_2 = 0.13, a_3 = 3.3, a_4 = 4.3, h = 0.7$, coefficient $k_{\rm GRB} = 10^{-8}[M_\odot{}^{-1}]$ (Fig. 8, light blue line). But according to our modeling of GRB as PISN it is natural to propose that the rate of GRB is equal (or is proportional) to the rate of PISN: $R_{\rm GRB} = R_{\rm PISN}$.

In this case we have used the rate of PISN from [61] Fig. 8, red line.

For our computation, we have supposed that at low z the GRB rate follows the result of [60], while at higher z we compute a rate using the relation of [61]. The sum of these two rates is represented in Figure 8.

Based on these simple assumptions we were able to compute the number of observed GRBs with redshift and compare it with observational data (the yellow histogram is the data of Swift). It was shown that general behavior is reproduced, but there are certainly some deviations. Apparently, GRBs do not trace star formation rate. The difference becomes more significant for the redhift $z \geq 5$. The PISN model predicts an increase in the number of GRBs with higher redshift, since primordial stars have higher masses and PISN explosions were more frequent. Of course our computation is a crude estimate because not all PISNe will produce a GRB and we certainly need a correcting factor. However, this result could explain the unexpected rise of GRBs as a function of redshift observed by Swift [19].

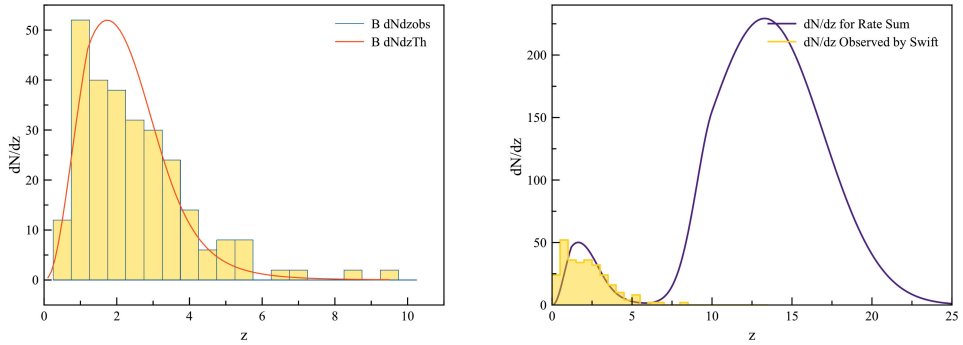


Figure 9 Left: Number of observed GRBs with redshift in $(z, z + dz)$ interval. Right: Number of observed GRBs with redshift in $(z, z + dz)$ interval and theoretical prediction at high z assuming that GRBs are related to PISNe.

4 A missing link in stellar evolution

The paradigm of gamma-ray burst is centralized on compactness problem and on the necessity of ultra-relativistic motion. This is the first ingredient of almost all GRB models. However, in a seminal paper, Ruderman introducing the physical problem of gamma-ray bursts did not exclude the possibility that different spikes might originate in different regions separated by larger distances [54]. It is interesting to see that Bussard and Lamb noticed also in 1982 that thermal Bremsstrahlung will need large area [55]. Therefore, we argue that the thermonuclear explosion is a possibility for GRB.

In another way, SN Ia are believed to be produced by thermonuclear explosion of white dwarfs are most luminous and often used as standard candles for measuring cosmological parameters. SNe Ibc and SNe II are generally thought to be produced by the core collapse of massive stars and are called core-collapse SNe. Long GRBs are also related to supernovae. The key question is how? How does a GRB engine work?

Here we have proposed a new paradigm of the pair instability supernovae explosion associated with GRBs. The key idea is the completely asymmetrical explosion of the star with fragmentation of the core. This is certainly the consequence of large scale convections associated with instabilities just before the explosion of the star, owing also to the strong temperature dependence of the nuclear reaction rates. Now, the central question of the validity of such scenario is more related to understanding of the PISNe explosion mechanism. Our scenario seems to be in contraction to many points related to the "standard fireball" scenario. Mazzali has found a mass range for GRB in 15–50 solar mass [62]. However, this mass is assuming a CC explosion and not a PISN. According to us, we think that the scenario of PISNe should be explored. If it is true that the core explodes in a completely asymmetric way with a complete mixing with envelope, then this will modify our standard vision of explosion of very massive stars. In some sense, GRBs could be a missing link in the stellar evolution which tells us this.

The main idea of our scenario is related to the new paradigm of the fragmentation of the core of the star during the explosion. We have presented a new paradigm of core fragmentation with is analogous to picture of fireworks where hundred of hot pieces are ejected in the explosion. Our 2D numerical simulations have shown that the fragmentation of the core could lead to similar results and therefore could explain naturally the GRB phenomena. If our scenario is correct, the lightcurves are simply a real picture of the explosion of a very massive star. Contrary to being a puzzling fact, the diversity of the light curve is the picture of the fragmentation of the core that could be tested using hydrodynamical codes in multidimensions: it is simply the DNA of the explosion.

Of course, this scenario is far from complete. But it proposes a complete coherent picture of a cosmic gamma ray burst. Inside this framework, the mass of the progenitor is the fundamental parameter as we have shown in the interpretation of the Amati relation: it gives an order of magnitude of the GRB budget: $E_{\rm nucl} \sim M_c \times q$. Now the value of energy peak in the spectrum is related to the average temperature of the star at the instant of the explosion: $E_{\rm peak} \sim T$. And the duration of the GRB, in our multi-sources paradigm is related to the size of the star $\Delta t \sim \frac{R}{c}$. The high value of mass for the GRB progenitor explains naturally the rate of GRB/SN without any model assumption. It is just a consequence of the Salpeter function. Finally exploring the cosmological consequences of the GRB we suggest that the rising part of the GRB rate with redshift is simply the tip of the iceberg of the PSINe–GRB connection we are starting to see at high redshift. Now will all PISN produce a GRB? Certainly not. Our model is certainly very simple and we have not taken into account the role of metallicity.

Acknowledgments

A. Filina thanks the European Commission, under the Grant Number 2012-1710 from the EACEA of the European Commission for financial supports. The research has received funding from the European Research Council under the European Union's Seventh Framework. V.M. Chechetkin thanks the Russian Science Foundation for Grant Number 16-11-10339. Pascal Chardonnet would like to thank the organizers of the Ioffe Workshop on Gamma-Ray Bursts.

References

[1] I. B. Strong, R. W. Klebesadel, & R. A. Olson, *ApJL* **188**, L1 (1974).
[2] I. B. Strong & R. W. Klebesadel, *Nature* **251**, 396 (1974).
[3] M. Schmidt, *Nature* **197**, 1040 (1963).
[4] A. Hewish, *Nature* **217**, 709 (1968).
[5] Z. Barkat, G. Rakavy, & N. Sack, *Phys. Rev. Lett.* **18**, 379 (1967).
[6] N. Gehrels & S. Razzaque, *Frontiers of Physics* **8**, 661 (2013).
[7] D. Band, J. Matteson, L. Ford, et al., *ApJ* **413**, 281 (1993).

[8] F. Frontera, Proceeding GRB in the afterglow era, *SP Conference Series* **312**, 10 (2003).
[9] E. Costa et al., *Nature* **387**, 783 (1997).
[10] J. van Paradijs et al., *Nature* **386**, 868 (1997).
[11] S. G. Djorgovski et al., *Nature* **387**, 876 (1997).
[12] M. R. Metzger et al., *Nature* **387**, 878 (1997).
[13] E. Galama et al., *Nature* **395**, 670 (1998).
[14] R. L. C. Starling et al., *A&A* **442**, L21 (2005).
[15] C. C. Thone et al., *ApJ* **676**, 1151 (2008).
[16] A. S. Fruckter et al., *Nature* **441**, 463 (2006).
[17] L. Christensen, J. Hjorth, & J. Gorosabel, *A&A* **425**, 913 (2004).
[18] M. Modjaz et al., *AJ* **135**, 1136 (2008).
[19] M. D. Kistler et al., *ApJL* **673**, 119 (2008).
[20] A. D. Falcone et al., *ApJ* **641**, 1010 (2006).
[21] S. A. Colgate *ApJ* **187**, 333 (1974).
[22] G. Bisnovatyi-Kogan et al. *Preprint, Institute of Applied Mathematics*, Moscow, USSR (1974).
[23] B. Paczynski, *ApJL* **494**, 45 (1998).
[24] S. Woosley, *ApJ* **405**, 273 (1993).
[25] A. I. MacFadyen & S. Woosley, *ApJ* **524**, 262 (1999).
[26] R. Ruffini et al., *ApJ* **555**, L107, L113, L119 (2001).
[27] P. Chardonnet, V. M. Chechetkin, & L. Titarchuk, *Astrophysics and Space Sciences* **325**, 153 (2010).
[28] W. A. Fowler & F. Hoyle, *ApJS* **9**, 201 (1964).
[29] G. Rakavy & G. Shaviv, *ApJ* **148**, 803 (1967).
[30] G. Rakavy et al., *ApJ* **150**, 131 (1967).
[31] G. Rakavy & G. Shaviv, *ApJSS* **1**, 429 (1968).
[32] G. S. Fraley, *ApJSS* **2**, 96 (1968).
[33] J. C. Wheeler, *ApJSS* **50**, 125 (1977).
[34] M. F. El Eid et al., *A&A* **119**, 54 (1983).
[35] W. W Ober et al., *A&A* **119**, 61 (1983).
[36] J. R. Bond et al., *ApJ* **280**, 825 (1984).
[37] W. Glatzel et al., *A&A* **149**, 413 (1985).
[38] A. A. Baranov, P. Chardonnet, V. M. Chechetkin, A. A. Filina, & M. V. Popov, *A&A*, **558**, AA10 (2013).
[39] L. Amati, *A&A* **390**, 81 (2002).
[40] P. Chardonnet, *IAU Symposium 250* **Poster presentation**, (2007).
[41] P. Chardonnet et al., *Cesar Lattes Meeting* **Rio de Janeiro**, (2015).
[42] Y. Kaneko, R. D. Preece, M. S. Briggs, et al., *ApJS* **166**, 298 (2006).
[43] L. Amati et al., *A&A* **508**, 173 (2009).
[44] U. Anzer & G. Boerner, *Mitteilungen der Astronomischen Gesellschaft Hamburg*, 38, 121 (1976).
[45] R. D. Preece, M. S. Briggs, R. S. Mallozzi, et al., 1998, *ApJL* **506**, L23
[46] J. Greene, *ApJ* **130**, 693 (1959).
[47] P. J. Brussaard & H. C. van de Hulst, *Reviews of Modern Physics* **34** , 507 (1962).
[48] L. Izzo, R. Ruffini, A. V. Penacchioni et al., *A&A* **543**, A10 (2012).
[49] F. Frontera, L. Amati, G. Guidorzi, R. Landi, & J. in't Zand, *ApJ* **754**, 138 (2012).

[50] F. Frontera, L. Amati, R. Farinelli, et al., *ApJ* **779**, 175 (2013).
[51] E. P. Mazets, & S. V. Golenetskii, *Astrophysics and Space Physics Reviews* **1**, 205 (1981).
[52] A. K. Harding, *Physics Report* **206**, 206, 327 (1991).
[53] J. P. Norris, G. H. Share, D. C. Messina, et al., *ApJ* **301**, 213 (1986).
[54] M. Ruderman, *Seventh Texas Symposium on Relativistic Astrophysics* **262**, 164 (1975).
[55] R. W. Bussard, & F. K. Lamb, *Gamma Ray Transients and Related Astrophysical Phenomena* **77**, 189 (1982).
[56] M. Khokhlov, *Astrophysics and Space Science Reviews* **8**,1 (1989).
[57] M. Della Valle, *The Twelfth Marcel Grossmann Meeting, Part A* 261 (2009).
[58] D. Wanderman & T. Piran, *MNRAS*, **406**, 1944 (2010).
[59] M. A. Campisi et al., *MNRAS*, **407**, 1972 (2010).
[60] A. M. Hopkins & J. F. Beacom, *ApJ* **651**, 142 (2006).
[61] J. A. Hummel et al., *ApJ*, **755**, 72 (2009).
[62] P A. Mazzali, *ApJ*, International Astronomical Union Meeting **279**, 75 (2012).